PHYSICAL REVIEW D **96,** 114509 (2017)

Electromagnetic form factors at large momenta from lattice QCD

A. J. Chambers,[1,*] J. Dragos,[1,2] R. Horsley,[3] Y. Nakamura,[4] H. Perlt,[5] D. Pleiter,[6,7] P. E. L. Rakow,[8] G. Schierholz,[9] A. Schiller,[5] K. Somfleth,[1] H. Stüben,[10] R. D. Young,[1] and J. M. Zanotti[1]

(QCDSF/UKQCD/CSSM Collaborations)

[1]*CSSM, Department of Physics, University of Adelaide, Adelaide, South Australia 5005, Australia*
[2]*National Superconducting Cyclotron Laboratory and Department of Physics and Astronomy, Michigan State University, East Lansing, Michigan 48824, USA*
[3]*School of Physics and Astronomy, University of Edinburgh, Edinburgh EH9 3JZ, United Kingdom*
[4]*RIKEN Advanced Institute for Computational Science, Kobe, Hyogo 650-0047, Japan*
[5]*Institut für Theoretische Physik, Universität Leipzig, 04103 Leipzig, Germany*
[6]*JSC, Jülich Research Centre, 52425 Jülich, Germany*
[7]*Institut für Theoretische Physik, Universität Regensburg, 93040 Regensburg, Germany*
[8]*Theoretical Physics Division, Department of Mathematical Sciences, University of Liverpool, Liverpool L69 3BX, United Kingdom*
[9]*Deutsches Elektronen-Synchrotron DESY, 22603 Hamburg, Germany*
[10]*Regionales Rechenzentrum, Universität Hamburg, 20146 Hamburg, Germany*

(Received 1 March 2017; revised manuscript received 29 June 2017; published 26 December 2017)

Accessing hadronic form factors at large momentum transfers has traditionally presented a challenge for lattice QCD simulations. Here, we demonstrate how a novel implementation of the Feynman-Hellmann method can be employed to calculate hadronic form factors in lattice QCD at momenta much higher than previously accessible. Our simulations are performed on a single set of gauge configurations with three flavors of degenerate mass quarks corresponding to $m_\pi \approx 470$ MeV. We are able to determine the electromagnetic form factors of the pion and nucleon up to approximately 6 GeV^2, with results for the ratio of the electric and magnetic form factors of the proton at our simulated quark mass agreeing well with experimental results.

DOI: 10.1103/PhysRevD.96.114509

I. INTRODUCTION

One of the great challenges of hadron physics is to build consistent and informative pictures of the internal structures of strongly interacting particles. An important aspect of this endeavor is the calculation of electromagnetic form factors for various baryons and mesons. These encode a description of the distribution of electromagnetic currents in hadrons and are key to describing the extended structure of these composite states.

For most of the second half of the 20th century, measurements of the electromagnetic form factors of the nucleon were obtained using the Rosenbluth separation technique [1] (also e.g. Ref. [2]). Broadly, these experiments indicated that the electric and magnetic form factors scaled proportionally for Q^2 up to around 6 GeV^2, with $\mu_p G_E^p/G_M^p \approx 1$ (where μ_p is the magnetic moment of the proton). This was later found to be in disagreement with recoil polarization experiments at Jefferson Lab, which showed $\mu_p G_E^p/G_M^p$ decreasing approximately linearly for $Q^2 \gtrsim 0.5$ GeV^2 (see e.g. Refs. [3–7]). This discrepancy is now largely understood through studies of two-photon exchange effects in the Rosenbluth method [8,9]. Nevertheless, it is still unknown whether the linear Q^2 trend continues and crosses zero or if the fall-off with Q^2 slows down. This has important consequences for our understanding of nucleon structure (see e.g. Refs. [10–13]). Experimental results are so far unable to obtain precise results at the relevant momentum scales, and so this remains an open question. Resolving the scaling of the form factors in this domain is one of the key physics goals of the upgraded continuous electron beam accelerator facility at Jefferson Lab.

The large-Q^2 behavior of the pion electromagnetic form factor F_π has proven challenging to probe experimentally—see Refs. [14–16] for recent innovative advances. Besides providing information about the electromagnetic structure of the pion, the Q^2-behavior of F_π provides insight into the transition from the soft to the hard regime in QCD (see Ref. [17] for a recent example). Owing to the present limitations, experimental data are unable to reliably discriminate different models describing the transition to the asymptotic domain [18].

*alexander.chambers@adelaide.edu.au

Lattice QCD calculations of hadronic form factors have typically focused on the study of processes at low-momentum transfer (see e.g. Refs. [19–24]), with only limited studies at large $Q^2 \gtrsim 3$ GeV^2 [25,26]. There is a variety of reasons that have contributed to the difficulty in accessing high-momentum transfer in lattice QCD. Given that the form factors fall with Q^2, it is immediately clear that one is attempting to extract a much weaker signal from data sets obtained with finite statistics. Further, in terms of the numerical computation, the signal-to-noise ratio of hadron correlators rapidly deteriorates as the momentum of the state is increased. This had commonly led to the study of three-point correlators which are projected to zero momentum at the hadron sink. In this case, the possible momentum transfers are limited by the maximum momentum available at the source. With limited statistical signal, it is therefore difficult to assess the degree of excited-state contamination, which can lead to significant systematic uncertainty [23,25,27–29].

In the present work, we demonstrate the ability to access high-momentum transfer in hadron form factors in lattice QCD using an extension of the Feynman-Hellmann theorem to nonforward matrix elements. This builds upon recent applications of the Feynman-Hellmann theorem for hadronic matrix elements in lattice QCD [30–33]—see also Refs. [34–41] for similar related techniques. Through the Feynman-Hellmann theorem, one relates matrix elements to energy shifts. In the case of lattice QCD, this allows one to access matrix elements from two-point correlators, rather than a more complicated analysis of three-point functions. This greatly simplifies the process of neutralizing excited-state contamination. As described below, the method most naturally works in the Breit frame $[E(\boldsymbol{p}') = E(\boldsymbol{p})]$, and hence one maximizes the momentum transfer for any given accessible state momentum $|\mathbf{p}|$. Finally, the high degree of correlations in the gauge ensembles makes it possible to extract a weak signal from a relatively noisy state.

Although this method is introduced in the calculation of electromagnetic form factors, the method is more broadly applicable to other nonforward hadronic matrix elements. The method could immediately be employed to determine axial form factors of hadrons or nuclei at high momentum transfer, for example. These quantities are particularly relevant for high-energy neutrino-nucleus scattering experiments. Extensions of the method recently published in Ref. [42] use second derivatives of the energy to calculate nucleon structure functions.

II. FEYNMAN-HELLMANN METHODS

Here we present briefly the extension of the Feynman-Hellmann method to nonforward matrix elements. For more detailed discussions of the Feynman-Hellmann theorem in lattice QCD, see e.g. Refs. [31,41]. To extend the Feynman-Hellmann analysis to nonforward matrix elements, we first consider a simple quantum mechanical situation. The familiar form of the Feynman-Hellmann theorem reads

$$\frac{\partial E_\psi}{\partial \lambda} = \left\langle \psi \middle| \frac{\partial H}{\partial \lambda} \middle| \psi \right\rangle, \tag{1}$$

where E is the energy eigenvalue of the state ψ. This readily follows from first-order perturbation theory. In the presence of spatially varying external fields, the conventional theorem requires a slight modification. We consider some first-order perturbation of the Hamiltonian, $H = H_0 + \lambda V$, which couples to a definite (real) spatial Fourier component,

$$\frac{\partial H}{\partial \lambda} \equiv \tilde{V}_+(\boldsymbol{q}) = \tilde{V}(\boldsymbol{q}) + \tilde{V}(-\boldsymbol{q}), \tag{2}$$

defined in terms of the complex Fourier modes $\tilde{V}(\boldsymbol{q}) = \int \mathrm{d}^3\boldsymbol{y} e^{i\boldsymbol{q}.\boldsymbol{y}} V(\boldsymbol{y})$, for some Hermitian potential $V(\boldsymbol{y})$. Note that periodicity of these fields on the lattice is ensured by the choice of lattice Fourier modes (see Ref. [43] for a discussion of more general implementations of momentum-dependent background fields). The diagonal matrix elements of this operator vanish in the basis of definite momentum eigenstates

$$\langle \boldsymbol{p} | \tilde{V}_+(\boldsymbol{q}) | \boldsymbol{p} \rangle = 0, \tag{3}$$

and standard perturbation theory would suggest that there is no shift of the energy level at first order in λ. The exception to this rule is in the case of a degeneracy in the unperturbed eigenstates $E_0(\boldsymbol{p}) = E_0(\boldsymbol{p} \pm \boldsymbol{q})$. The familiar solution in this case is to invoke degenerate perturbation theory where one diagonalizes the space of the degeneracy with respect to the applied external potential. The degeneracy condition dictates that one is considering Breit-frame transitions. For demonstrative purposes, we choose the simple case in which $\boldsymbol{p} = \pm\boldsymbol{q}/2$, and hence at lowest order in the field strength the system is diagonalized by the states $|\boldsymbol{q}/2\rangle_\pm \propto |\boldsymbol{q}/2\rangle \pm |-\boldsymbol{q}/2\rangle$. The corresponding eigenvalues are given by $E_0(\boldsymbol{q}/\boldsymbol{2}) \pm \lambda\Delta E + \mathcal{O}(\lambda^2)$, where the energy shift corresponds to the matrix element of interest,

$$\Delta E = {}_+\langle \boldsymbol{q}/2 | \tilde{V}_+(\boldsymbol{q}) | \boldsymbol{q}/2 \rangle_+ = \langle \boldsymbol{q}/2 | \tilde{V}(\boldsymbol{q}) | -\boldsymbol{q}/2 \rangle. \tag{4}$$

Owing to the discretized spectrum (and momentum) on the lattice, this quantum mechanical argument translates in a straightforward fashion to hadronic matrix elements. In the case of continuous momenta, the presence of the periodic potential induces a gap in the dispersion curve, as in conventional band theory.

To implement within a lattice QCD calculation, the Lagrangian is modified to incorporate a spatially varying external potential,

$$\mathcal{L}(y) \to \mathcal{L}(y) + \lambda(e^{+i\boldsymbol{q}\cdot\boldsymbol{y}} + e^{-i\boldsymbol{q}\cdot\boldsymbol{y}})\mathcal{O}(y), \tag{5}$$

where the phase of the exponentials is defined with respect to the location of the hadron source at $\boldsymbol{y} = \boldsymbol{0}$. The symbol $\mathcal{O}$ denotes a quark-bilinear operator, and λ represents the strength of the external field—which is kept small to ensure that the energy response is in the linear regime. Alternatively, one may isolate the linear λ dependence of the correlator directly by constructing compound propagators [40,41].

To compute connected quark contributions, quark propagators are inverted according the modified action corresponding to Eq. (5)—sea-quark contributions would require new gauge ensembles [33] or an effective reweighting technique. Fourier-projected, hadron correlation functions are defined by

$$C^{\lambda}_{\boldsymbol{p}}(t) = \sum_{\boldsymbol{x}} e^{-i\boldsymbol{p}\cdot\boldsymbol{x}}{}_{\lambda}\langle\Omega|\chi(t,\boldsymbol{x})\chi^{\dagger}(0,\boldsymbol{0})|\Omega\rangle_{\lambda}, \tag{6}$$

where subscript $|\Omega\rangle_{\lambda}$ is the vacuum of the modified theory. The spectrum can be directly isolated by constructing even and odd linear combinations,

$$C^{\lambda\pm}_{\boldsymbol{p},\boldsymbol{p}'} = C^{\lambda}_{\boldsymbol{p}} \pm C^{\lambda}_{\boldsymbol{p}'}, \tag{7}$$

of Breit-frame momentum pairs, $\boldsymbol{p}$ and $\boldsymbol{p}'(=\boldsymbol{p}+\boldsymbol{q})$. To isolate an energy shift, it is more straightforward to implement the "+" combination $C^{\lambda+}_{\boldsymbol{p},\boldsymbol{p}'}$ rather than the "−" sum, which vanishes in the free-field limit.

Only the Breit-frame pairs will receive an energy shift which is linear in the applied field strength λ. This energy shift corresponds directly to the hadronic matrix element of interest,

$$\left.\frac{\partial E_H(\boldsymbol{p}')}{\partial\lambda}\right|_{\lambda=0} = \frac{\langle H(\boldsymbol{p}')|\mathcal{O}(0)|H(\boldsymbol{p})\rangle}{\langle H(\boldsymbol{p}')|H(\boldsymbol{p}')\rangle}, \tag{8}$$

or similarly for $\boldsymbol{p} \leftrightarrow \boldsymbol{p}'$. We have confirmed numerically that non–Breit frame states do not receive a linear energy response, as expected.

III. SIMULATION DETAILS

In the present work, we use an ensemble of 1700 gauge-field configurations with $2+1$ flavors of nonperturbatively $O(a)$-improved Wilson fermions and a volume $L^3 \times T = 32^3 \times 64$. The lattice spacing $a = 0.074(2)$ fm is set using a number of singlet quantities [44–47]. We use hopping parameters $(\kappa_l, \kappa_s) = (0.120900, 0.120900)$, which correspond to a pion mass of ∼470 MeV. The clover action used comprises the tree-level Symanzik-improved gluon action together with a stout smeared fermion action, modified for the implementation of the Feynman-Hellmann method [31].

TABLE I. Momentum insertions and the corresponding Breit-frame momenta used in these calculations, where $\boldsymbol{p}' = -\boldsymbol{p}$. Momenta are given in lattice Fourier units of $2\pi/L$.

$\boldsymbol{q}$	$\boldsymbol{p}$	$\boldsymbol{p}^2$	Q^2
(0,0,0)	(0,0,0)	0	0
(2,0,0)	(1,0,0)	1	4
(2,2,0)	(1,1,0)	2	8
(2,2,2)	(1,1,1)	3	12
(4,0,0)	(2,0,0)	4	16
(4,2,0)	(2,1,0)	5	20
(4,2,2)	(2,1,1)	6	24

To study electromagnetic form factors, quark propagators are calculated by inverting a modified Dirac matrix, determined by the Lagrangian

$$\mathcal{L}(y) \to \mathcal{L}(y) + (e^{+i\boldsymbol{q}\cdot\boldsymbol{y}} + e^{-i\boldsymbol{q}\cdot\boldsymbol{y}})\bar{q}(y)\lambda\cdot\gamma q(y). \tag{9}$$

Here, either λ_2 or λ_4 takes nonzero values of 1×10^{-4} or -1×10^{-5}, and the values of $\boldsymbol{q}$ are listed in Table I. Note that we only use the simplest Breit-frame kinematics, $\boldsymbol{p}' = -\boldsymbol{p}$. This choice allows us to minimize $\boldsymbol{p}^2$ for each value of $\boldsymbol{q}^2$ and hence minimize the noise in the correlator. As described below, this also projects the nucleon energy shifts directly onto G_E or G_M. A single source is used on each of the 1700 gauge configurations for each value of $\boldsymbol{q}$. We note that once an unmodified Dirac matrix has been inverted ($\lambda = 0$), the solution provides an excellent guess for the $\lambda \neq 0$-quark propagators, for small values of the coupling. As such, each subsequent inversion of a modified Dirac matrix only costs an additional 20%–30% over the initial $\lambda = 0$ propagator.

IV. RESULTS

A. Electromagnetic form factors of the nucleon

The (Euclidean) decomposition of the vector current for the individual quark flavor contributions of the nucleon is written in terms of the familiar Dirac and Pauli (F_1^q and F_2^q) form factors,

$$\langle N(p',s')|\bar{q}(0)\gamma_\mu q(0)|N(p,s)\rangle = \bar{u}(p',s')\left[\gamma_\mu F_1^q(Q^2) + \frac{\sigma_{\mu\nu}q_\nu}{2M_N}F_2^q(Q^2)\right]u(p,s), \tag{10}$$

where we denote the invariant 4-momentum transfer squared as $Q^2 = -q^2 = -(p'-p)^2$. The Sachs electromagnetic form factors are defined by

$$G_E^q = F_1^q - \frac{Q^2}{(2M)^2}F_2^q \tag{11}$$

$$G_M^q = F_1^q + F_2^q. \tag{12}$$

For the incident-normal Breit frame ($\boldsymbol{p}' = -\boldsymbol{p}$), the temporal and spatial components of the current give rise

to energy shifts which directly project out the electric and magnetic form factors respectively,

$$\left.\frac{\partial E_N}{\partial \lambda_4}\right|_{\lambda=0} \overset{p'=-p}{=} \frac{M_N}{E_N} G_E^q, \tag{13}$$

$$\left.\frac{\partial E_N}{\partial \lambda_i}\right|_{\lambda=0} \overset{p'=-p}{=} \frac{[\hat{e}\times q]_i}{2E_N} G_M^q, \tag{14}$$

where $\hat{e}$ is the unit-normalized spin polarization vector of the nucleon state determined by the Dirac projector.

$$\Gamma(e) \equiv \frac{1}{2}(\mathrm{I} - i\hat{e}\cdot\gamma\gamma_5). \tag{15}$$

In our calculations, $\hat{e} \equiv (0,0,1)$.

Utilizing ratios of correlators with and without the applied external field, we can define "effective form factors" by appropriate scaling of the effective energy shift $\Delta E_{N\mathrm{eff}}$.,

$$G^q_{E(\mathrm{eff})} = \frac{E_N}{M_N}\frac{\Delta E_{N(\mathrm{eff})}}{\lambda}, \tag{16}$$

$$G^q_{M(\mathrm{eff})} = \frac{2E_N}{[\hat{e}\times q]_i}\frac{\Delta E_{N(\mathrm{eff})}}{\lambda_i}, \tag{17}$$

where the effective energy is defined in the usual way in terms of lattice correlation functions G,

$$E_{N\mathrm{eff}}\left(t+\frac{a}{2}\right) = \frac{1}{a}\ln\left|\frac{G(t)}{G(t+a)}\right|. \tag{18}$$

The effective form factors should plateau to the relevant form factors provided λ is small enough that the energy shift is predominantly linear. Figure 1 shows results for effective electromagnetic form factors for a subset of Q^2 values. We note that for the λ values chosen, the signals are statistically identical, indicating we are indeed in the linear regime. We identify that quite clean plateaux are realized up to a quite large momentum transfer. As a check on the selected fit window, we ensure that the free-field correlators are sufficiently saturating to the ground-state energy dispersion. Figure 2 shows the raw energy shifts as a function of λ for three different values of Q^2 and further emphasizes that we are most definitely in the linear regime.

Figure 3 shows results for the proton electric and magnetic form factors—neglecting disconnected contributions, which are anticipated to be very small at large Q^2 [48]. In the low-Q^2 region, we compare with results computed on the same ensembles using a variationally improved three-point function approach, as described in Ref. [29]. The experimental parametrization of Ref. [49] is also included and demonstrates the effect of the unphysical quark mass in the dropoff of the form factors. Very good agreement is observed between the two different lattice

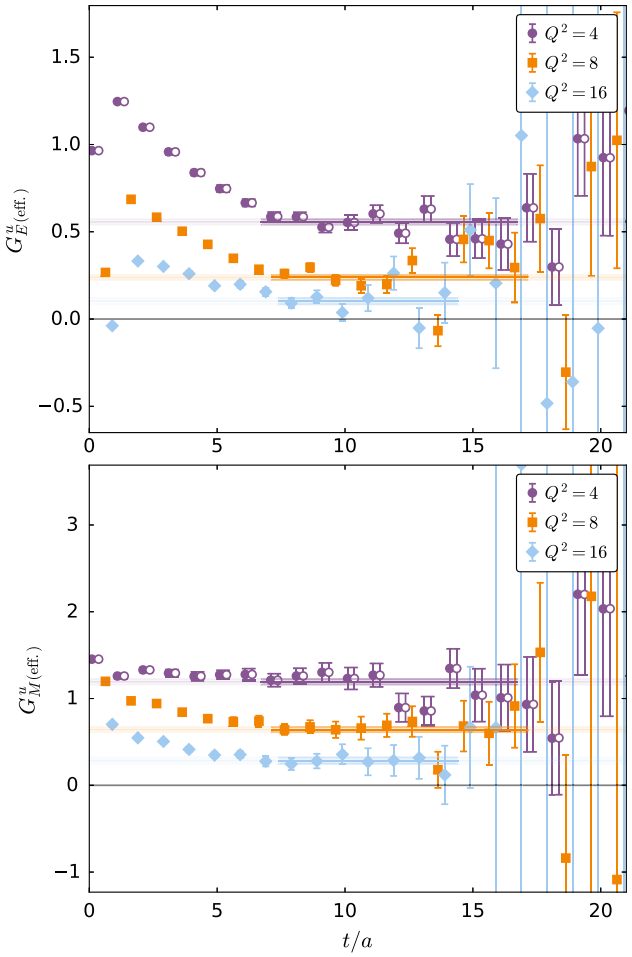

FIG. 1. Effective electric and magnetic form factors of the u quark in the nucleon for different values of Q^2. Results for $Q^2 = 4$ are shown for both values of λ (10^{-4} and -10^{-5}).

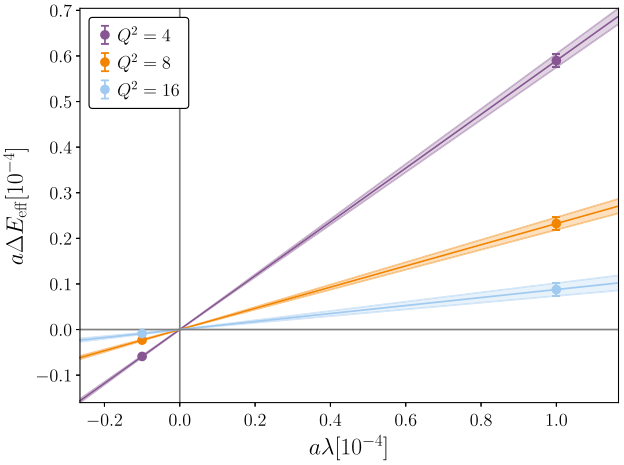

FIG. 2. Nucleon energy shift as a function of λ when the u-quark Lagrangian is modified to include a coupling to the temporal component of the vector current, for the calculation of G_E.

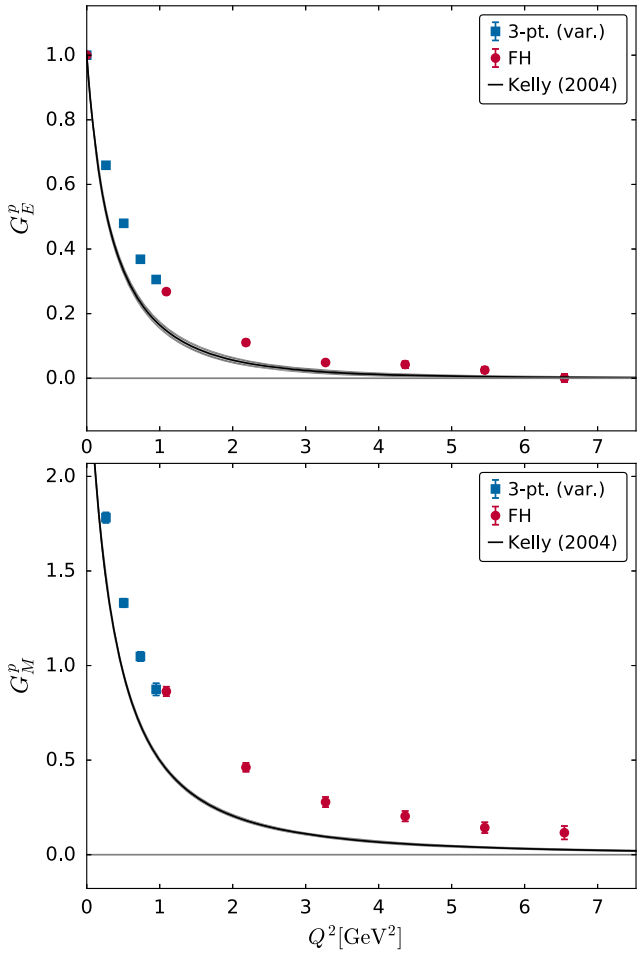

FIG. 3. G_E and G_M for the proton from the Feynman-Hellmann method and from a variational method described in Ref. [29] employed on the same ensemble. The experimental parametrization is from Ref. [49].

QCD calculations in the region of overlap. The statistical signal for the new Feynman-Hellmann approach is seen to extend to much larger Q^2 than has been accessible in the past. Phenomenologically, the Q^2 range we are now able to access would allow for tighter constraints to be placed on the distribution of charge and magnetization in the nucleon at small impact parameter [50].

Figure 4 displays the extraction of the ratio G_E/G_M for the proton as a function of Q^2 and a comparison to experiment [5–7]. Unlike early analyses of form factors, which suggested a constant G_E/G_M, our results show a general trend to fall off at larger Q^2 (at this quark mass), as seen in modern double-polarization measurements [3–7]. This is somewhat surprising given the unphysical simulated pion mass of 470 MeV and suggests that the quark mass dependence of this ratio warrants further study.

B. Electromagnetic form factor of the pion

Following an analysis similar to that for the nucleon, we show the determination of the pion form factor and

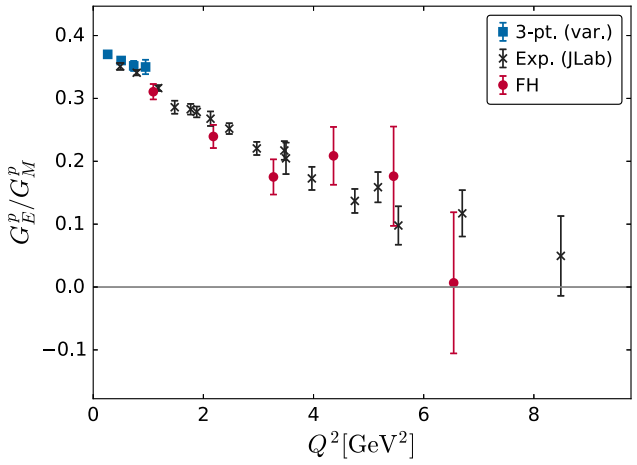

FIG. 4. Ratio G_E/G_M for the proton from the application of the Feynman-Hellmann method, from a variational analysis of three-point functions [29], and from experiment [5–7]. Note this is not scaled by the magnetic moment of the proton μ_p, as this would require phenomenological fits to the low-Q^2 data, which is not the focus of this work.

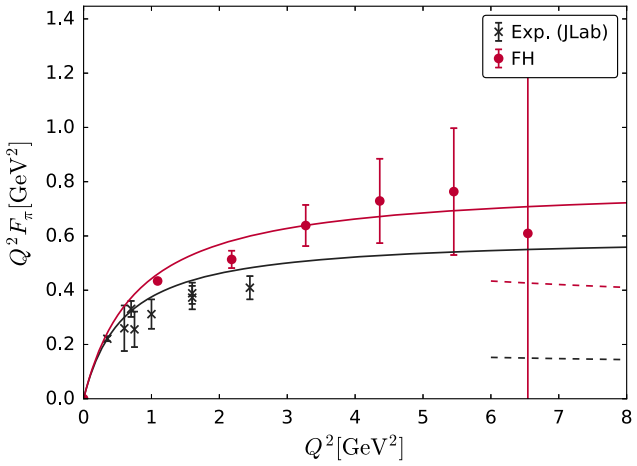

FIG. 5. Scaled pion form factor Q^2F_π from the Feynman-Hellmann technique and from experiment [16]. The solid lines are the vector meson dominance at the relevant pion masses, and the dotted lines are the asymptotic values predicted by perturbative QCD (see [17] for a discussion of this value and its limitations).

comparison to experiment [16] in Fig. 5. The realized statistical signal gives confidence that future lattice QCD simulations will be able to provide important insight into this transition between the perturbative and nonperturbative regimes.

V. CONCLUSION

In this work, we have extended the Feynman-Hellmann technique to access nonforward matrix elements. We demonstrate that this provides for a dramatic improvement in the ability to extract nucleon and pion form factors at much

higher momentum transfers than previously possible. Before making rigorous comparisons with phenomenology, standard lattice systematics must be further quantified, including quark mass dependence, discretization artifacts, and continuum extrapolation. There is also further potential for increased precision by using improved operators that have better access to high-momentum states, as proposed in Ref. [51].

The high-momentum form factors extracted in this work demonstrate a significantly expanded scope for lattice QCD to address this phenomenologically interesting domain of hadron structure and opens up a vista of possibilities for determining other hadronic and nuclear quantities at high momentum transfer.

ACKNOWLEDGMENTS

The numerical configuration generation was performed using the BQCD lattice QCD program [52], on the IBM BlueGeneQ using DIRAC 2 resources (EPCC, Edinburgh, United Kingdom), the BlueGene P and Q at NIC (Jülich, Germany), and the Cray XC30 at HLRN (Berlin-Hannover, Germany). Some of the simulations were undertaken using resources awarded at the NCI National Facility in Canberra, Australia, and the iVEC facilities at the Pawsey Supercomputing Centre. These resources are provided through the National Computational Merit Allocation Scheme and the University of Adelaide Partner Share supported by the Australian Government. This work was supported in part through supercomputing resources provided by the Phoenix HPC service at the University of Adelaide. The BlueGene codes were optimized using Bagel [53]. The CHROMA software library [54] was used in the data analysis. A. J. C. was supported by the Australian Government Research Training Program Scholarship. J. D. gratefully acknowledges support by the National Superconducting Cyclotron Laboratory/Facility for Rare Isotope Beams and Michigan State University during the preparation of this work. G. S. was supported by DFG Grant No. SCHI 179/8-1. H. P. was supported by DFG Grant No. SCHI 422/10-1. This investigation has been supported by the Australian Research Council under Grants No. FT120100821, No. FT100100005, and No. DP140103067 (R. D. Y. and J. M. Z.).

[1] M. N. Rosenbluth, Phys. Rev. **79**, 615 (1950).
[2] I. A. Qattan *et al.*, Phys. Rev. Lett. **94**, 142301 (2005).
[3] M. K. Jones *et al.* (Jefferson Lab Hall A Collaboration), Phys. Rev. Lett. **84**, 1398 (2000).
[4] O. Gayou *et al.* (Jefferson Lab Hall A Collaboration), Phys. Rev. Lett. **88**, 092301 (2002).
[5] V. Punjabi *et al.*, Phys. Rev. C **71**, 055202 (2005); **71**, 069902(E) (2005).
[6] A. J. R. Puckett *et al.*, Phys. Rev. Lett. **104**, 242301 (2010).
[7] A. J. R. Puckett *et al.*, Phys. Rev. C **85**, 045203 (2012).
[8] P. A. M. Guichon and M. Vanderhaeghen, Phys. Rev. Lett. **91**, 142303 (2003).
[9] P. G. Blunden, W. Melnitchouk, and J. A. Tjon, Phys. Rev. C **72**, 034612 (2005).
[10] G. A. Miller, Phys. Rev. Lett. **99**, 112001 (2007).
[11] I. C. Cloët, G. Eichmann, B. El-Bennich, T. Klahn, and C. D. Roberts, Few-Body Syst. **46**, 1 (2009).
[12] I. C. Cloët, C. D. Roberts, and A. W. Thomas, Phys. Rev. Lett. **111**, 101803 (2013).
[13] R. S. Sufian, G. F. de Téramond, S. J. Brodsky, A. Deur, and H. G. Dosch, Phys. Rev. D **95**, 014011 (2017).
[14] J. Volmer *et al.* (Jefferson Lab F(pi) Collaboration), Phys. Rev. Lett. **86**, 1713 (2001).
[15] T. Horn *et al.* (Jefferson Lab F(pi)-2 Collaboration), Phys. Rev. Lett. **97**, 192001 (2006).
[16] G. M. Huber *et al.* (Jefferson Lab Collaboration), Phys. Rev. C **78**, 045203 (2008).
[17] L. Chang, I. C. Cloët, C. D. Roberts, S. M. Schmidt, and P. C. Tandy, Phys. Rev. Lett. **111**, 141802 (2013).
[18] T. Horn and C. D. Roberts, J. Phys. G **43**, 073001 (2016).
[19] S. Collins *et al.*, Phys. Rev. D **84**, 074507 (2011).
[20] C. Alexandrou, M. Brinet, J. Carbonell, M. Constantinou, P. A. Harraud, P. Guichon, K. Jansen, T. Korzec, and M. Papinutto, Phys. Rev. D **83**, 094502 (2011).
[21] P. E. Shanahan, A. W. Thomas, R. D. Young, J. M. Zanotti, R. Horsley, Y. Nakamura, D. Pleiter, P. E. L. Rakow, G. Schierholz, and H. Stüben (QCDSF/UKQCD and CSSM Collaborations), Phys. Rev. D **89**, 074511 (2014).
[22] P. E. Shanahan, A. W. Thomas, R. D. Young, J. M. Zanotti, R. Horsley, Y. Nakamura, D. Pleiter, P. E. L. Rakow, G. Schierholz, and H. Stüben, Phys. Rev. D **90**, 034502 (2014).
[23] J. R. Green, J. W. Negele, A. V. Pochinsky, S. N. Syritsyn, M. Engelhardt, and S. Krieg, Phys. Rev. D **90**, 074507 (2014).
[24] S. Capitani, M. D. Morte, D. Djukanovic, G. von Hippel, J. Hua, B. Jäger, B. Knippschild, H. B. Meyer, T. D. Rae, and H. Wittig, Phys. Rev. D **92**, 054511 (2015).
[25] H.-W. Lin, S. D. Cohen, R. G. Edwards, K. Orginos, and D. G. Richards, arXiv:1005.0799.
[26] J. Koponen, A. C. Zimermmane-Santos, C. T. H. Davies, G. P. Lepage, and A. T. Lytle, Phys. Rev. D **96**, 054501 (2017).
[27] B. J. Owen, J. Dragos, W. Kamleh, D. B. Leinweber, M. S. Mahbub, B. J. Menadue, and J. M. Zanotti, Phys. Lett. B **723**, 217 (2013).
[28] B. Yoon *et al.*, Phys. Rev. D **93**, 114506 (2016).
[29] J. Dragos, R. Horsley, W. Kamleh, D. B. Leinweber, Y. Nakamura, P. E. L. Rakow, G. Schierholz, R. D. Young, and J. M. Zanotti, Phys. Rev. D **94**, 074505 (2016).
[30] R. Horsley, R. Millo, Y. Nakamura, H. Perlt, D. Pleiter, P. E. L. Rakow, G. Schierholz, A. Schiller, F. Winter,

and J. M. Zanotti (UKQCD and QCDSF Collaborations), Phys. Lett. B **714**, 312 (2012).
[31] A. J. Chambers *et al.* (QCDSF/UKQCD and CSSM Collaborations), Phys. Rev. D **90**, 014510 (2014).
[32] A. J. Chambers, R. Horsley, Y. Nakamura, H. Perlt, P. E. L. Rakow, G. Schierholz, A. Schiller, and J. M. Zanotti (QCDSF Collaboration), Phys. Lett. B **740**, 30 (2015).
[33] A. J. Chambers *et al.*, Phys. Rev. D **92**, 114517 (2015).
[34] W. Detmold, Phys. Rev. D **71**, 054506 (2005).
[35] M. Engelhardt (LHPC Collaboration), Phys. Rev. D **76**, 114502 (2007).
[36] W. Detmold, B. C. Tiburzi, and A. Walker-Loud, Phys. Rev. D **79**, 094505 (2009).
[37] W. Detmold, B. C. Tiburzi, and A. Walker-Loud, Phys. Rev. D **81**, 054502 (2010).
[38] T. Primer, W. Kamleh, D. Leinweber, and M. Burkardt, Phys. Rev. D **89**, 034508 (2014).
[39] W. Freeman, A. Alexandru, M. Lujan, and F. X. Lee, Phys. Rev. D **90**, 054507 (2014).
[40] M. J. Savage, P. E. Shanahan, B. C. Tiburzi, M. L. Wagman, F. Winter, S. R. Beane, E. Chang, Z. Davoudi, W. Detmold, and K. Orginos, Phys. Rev. Lett. **119**, 062002 (2017).
[41] C. Bouchard, C. C. Chang, T. Kurth, K. Orginos, and A. Walker-Loud, Phys. Rev. D **96**, 014504 (2017).
[42] A. J. Chambers, R. Horsley, Y. Nakamura, H. Perlt, P. E. L. Rakow, G. Schierholz, A. Schiller, K. Somfleth, R. D. Young, and J. M. Zanotti, Phys. Rev. Lett. **118**, 242001 (2017).
[43] Z. Davoudi and W. Detmold, Phys. Rev. D **92**, 074506 (2015).
[44] R. Horsley, J. Najjar, Y. Nakamura, H. Perlt, D. Pleiter, P. E. L. Rakow, G. Schierholz, A. Schiller, H. Stüben, and J. M. Zanotti (QCDSF-UKQCD Collaboration), Proc. Sci., LATTICE2013 (**2013**) 249.
[45] V. G. Bornyakov *et al.*, arXiv:1508.05916.
[46] W. Bietenholz *et al.*, Phys. Lett. B **690**, 436 (2010).
[47] W. Bietenholz *et al.*, Phys. Rev. D **84**, 054509 (2011).
[48] J. Green, S. Meinel, M. Engelhardt, S. Krieg, J. Laeuchli, J. Negele, K. Orginos, A. Pochinsky, and S. Syritsyn, Phys. Rev. D **92**, 031501 (2015).
[49] J. J. Kelly, Phys. Rev. C **70**, 068202 (2004).
[50] S. Venkat, J. Arrington, G. A. Miller, and X. Zhan, Phys. Rev. C **83**, 015203 (2011).
[51] G. S. Bali, B. Lang, B. U. Musch, and A. Schäfer, Phys. Rev. D **93**, 094515 (2016).
[52] Y. Nakamura and H. Stüben, Proc. Sci., LATTICE2010 (**2010**) 040.
[53] P. A. Boyle, Comput. Phys. Commun. **180**, 2739 (2009).
[54] R. G. Edwards and B. Joo (SciDAC, LHPC, and UKQCD Collaborations), Nucl. Phys. B, Proc. Suppl. **140**, 832 (2005).